nature geoscience

LETTERS

PUBLISHED ONLINE: 16 JANUARY 2011 | DOI: 10.1038/NGEO1057

Influence of human and natural forcing on European seasonal temperatures

Gabriele Hegerl[1]*, Juerg Luterbacher[2], Fidel González-Rouco[3], Simon F. B. Tett[1], Thomas Crowley[1] and Elena Xoplaki[4]

It is the regional and seasonal expression of climate change that determines the effect of greenhouse warming on ecosystems and society[1]. Whereas anthropogenic influences on European temperatures have been detected over the twentieth century[2,3], it has been suggested that the impact of external influences on European temperatures before 1900 is negligible[4]. Here we use reconstructions of seasonal European land temperature[5,6] and simulations with three global climate models[7–9] to show that external influences on climate—such as the concentrations of stratospheric volcanic aerosols or greenhouse gases, other anthropogenic effects and possibly changes in total solar irradiance—have had a discernible influence on European temperatures throughout the past five centuries. In particular, we find that external forcing contributes significantly ($p < 5\%$) to the reconstructed long-term variability of winter and spring temperatures and that it is responsible for a best guess of 75% of the observed winter warming since the late seventeenth century. This warming is largely attributable to greenhouse-gas forcing. Summer temperatures show detectable ($p < 5\%$) interdecadal variations in response to external forcing before 1900 only. Finally, throughout the record we detect highly significant summer cooling and significant winter warming following volcanic eruptions.

Studies on the basis of instrumental data find a discernible anthropogenic contribution to twentieth-century annual[2] and seasonal European temperatures[10]. For the period before 1900, ref. 4 postulates that preindustrial European climate is 'fundamentally a consequence of internal fluctuations of the climate system'. This conclusion is based on the consistent variability found for short timescales in an unforced atmosphere–ocean general circulation model (AOGCM) control simulation and the reconstruction[5,6]. Although reconstructions of spatial patterns of past climate[11], together with models, provide suggestive information on mechanisms and forcings which contributed to past climate variability[12–14], detection and attribution studies have been limited to palaeoclimate reconstructions of Northern Hemispheric mean temperature[3,15]. The present availability of AOGCM forced simulations and climate field reconstructions also enables detection and attribution studies at finer, continental and seasonal scales.

Here we apply detection and attribution methods to seasonal reconstructions of European land temperature covering the period 1500–2000 (refs 5,6), to separate externally driven variability from internal fluctuations and to quantify the role of external forcing. The temperature reconstruction relies on information from early instrumental, documentary and natural proxy data before 1900; and instrumental data thereafter[5,6] see also Supplementary Information for detail). To account for the reduced data availability and increased non-temperature proxy noise before 1675 (which may lead to some loss of variance early in the reconstruction[16,17]) the analysis considers both the full 500 year period and the 1675–1999 subset.

We use data from the ECHO-G (refs 7,18); HadCM3 (ref. 8) and NCAR CSM1.4 (ref. 9) AOGCMs (see Supplementary Information for details) to estimate the expected response to external forcing and its signal-to-noise ratio when compared with the variability generated within the climate system. The model and reconstruction data have been transformed to the coarser ECHO-G and CSM1.4 grids and reduced to the European land domain (see Supplementary Information). Like the observations, simulations with climate models contain both the response to external forcing and dynamically induced internal climate variability. The responses of the three climate model simulations correlate on average more with one another in autumn and winter, suggesting a stronger role of external forcing during these seasons. The correlation is smaller in summer (Table 1). This is despite much stronger interannual and decadal variability occurring in the winter (Fig. 1, Supplementary Table S2), and suggests that radiative forcing shows a weaker influence during summer.

We applied a detection and attribution method to determine the role of external forcing in the reconstructed temperature variability of the past 500 years. The fingerprint for external forcing is based on the time evolution of the model-simulated European mean response to external drivers, as the spatial pattern of the reconstruction is less robust than the continental average. The method applies a total least square fit of this fingerprint to the reconstruction. The uncertainty in the fit is estimated by superimposing samples of internal climate variability, which are taken from climate-model data and also from the remaining, unexplained variability in the reconstruction. If the 5–95% uncertainty range of the scaling factor is above zero, then the role of forcing is significant ($p < 5\%$) (for more detail, see Methods). A similar method has been previously applied to reconstructions of hemispheric mean temperatures[15,19]. We find that the fingerprint of external forcing is detectable in winter, spring and annual mean European temperatures for 1500–1996 (Fig. 2, Table 1; 1996 cutoff owing to the length of some simulations used). Figure 2 shows that the detected winter and spring temperature changes in response to forcing include the cold conditions in the late seventeenth and early nineteenth centuries, which are interrupted by warming in the mid-eighteenth century in both reconstruction and fingerprint. A large fraction (best estimate 75%, with a 5–95% uncertainty

[1]School of GeoSciences, University of Edinburgh, West Mains Rd, Edinburgh EH9 3JW, UK, [2]Justus-Liebig University of Giessen, Department of Geography, Senckenbergstr. 1, D-35390 Giessen, Germany, [3]Universidad Complutense Madrid, Ciudad Universitaria, 28040 Madrid, Spain, [4]University of Bern, Institute of Geography and Oeschger Centre for Climate Change Research, Hallerstrasse 12, CH-3012 Bern, Switzerland. *e-mail: gabi.hegerl@ed.ac.uk.

 NATURE GEOSCIENCE DOI: 10.1038/NGEO1057

Table 1 | Detection and attribution results for seasonal- and area-average European temperature data 1500–1996.

	Best-guess scaling	5–95% range	Individual detectable signals	Corr. recon. r	Intermod. ave. corr.
Winter	**0.59**	**[0.34, 1.05]**	Anthro. $< 5\%$	0.51	0.28
Spring	**0.53**	**[0.27 1.15]**	Anthro. $\sim 10\%$	0.50	0.24
Summer	0.47	[−0.2 1.00]	Solar $\sim 5\%$, not robust	0.19	0.17
Su < 1900	**1.15**	**[0.20 1.98]**	Solar $\sim 5\%$, not robust	0.37	0.16
Autumn	**0.23***	**[0.00 0.71]**	-	0.37	0.39
Annual	**0.46***	**[0.19 0.84]**	-	0.59	0.37

First column, list of the scaling factors β (equation (1)) for individual seasons; second column, 5–95% uncertainty range. Note that ranges not encompassing zero show that the response to forcing is detectable (in bold), scaling factors that do not encompass unity yield results that need to be significantly scaled to match the observations (indicated by an asterisk). Third column, signals that are detectable in the multiregression (equation (2)) with significance level. Fourth column, correlation of the multimodel mean fingerprint with the reconstruction. Fifth column, average correlation between a single-model simulation and a fingerprint from both other simulations combined.

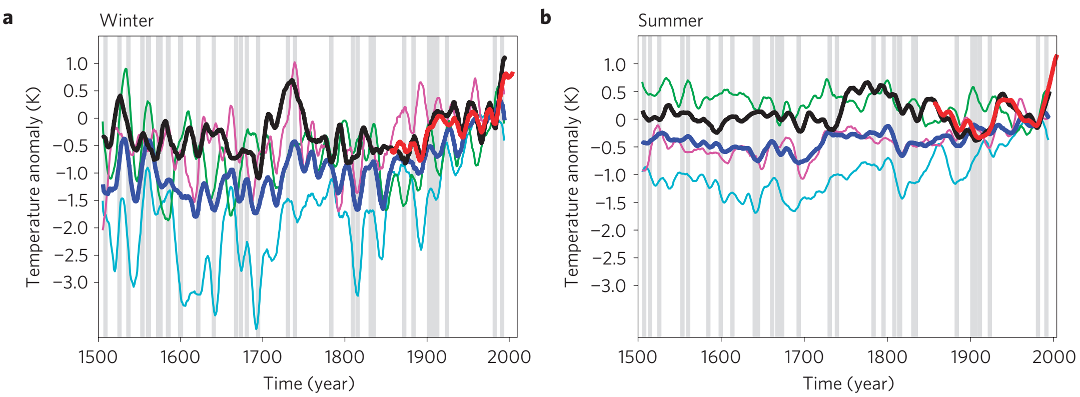

Figure 1 | Comparison between simulated and reconstructed European temperature anomalies (K with respect to the 1961–1990 climatology). Winter and summer temperature anomalies 1500–2000 from the reconstruction[5] are shown in black, instrumental data in red[30] and climate-model simulations in green (HadCM3; ref. 8), magenta (NCAR-CSM1.4; ref. 9) and cyan (ECHO-G; ref. 7). The multimodel mean is shown in bold dark blue. All data are smoothed by a filter emphasizing timescales beyond 15 years (11 and 7 year boxcar filters applied consecutively). Years with volcanic eruptions on the basis of ref. 23 are marked by grey bars.

range of 44–133%) of the reconstructed long-term winter warming between the second half of the seventeenth century (1651–1700) and the second half of the twentieth century (1951–1996) can be attributed to external forcing. This estimate is based on the multimodel-simulated warming over that period, multiplied by the 5–95% range of scaling factors that yield the models consistent with the reconstruction. This range accounts for the possibility that internal variability may have contributed to or counteracted the warming caused by the forcing. If the attribution analysis is based on winter data for the post-1675 period, or the period 1500–1950, results continue to show a significant response to all forcings. However, the response is no longer detectable if the analysis is carried out over the 1500–1900 period. This suggests that the overall winter warming into the twentieth century increases the signal-to-noise ratio of external forcing. The reconstruction for autumn shows significant, but small, detectable responses to external drivers (Table 1, Fig. 2). In summer, the fingerprint of external forcing is detected before 1900 (1500–1900 or 1675–1900; Table 1, Fig. 2), but no significant forcing is detected for the full 500 year period. It is unclear if uncertainties in forcing, including aerosols and land-use change[20], make detection of external forcing more difficult within the twentieth century. The model simulations considered involve different forcings in this later period and overall show low inter-model correlations in summer (Table 1). In contrast, very recent instrumental summer warming is highly unusual relative to the past: temperature trends over 30 years, starting with the trend 1971–2000, to the trend 1980–2009, are significantly ($p < 5\%$) larger than other summer trends from the 1675–1999 reconstructed record, or simulated records from individual-model simulations (see Supplementary Fig. S2). As these trends are in good agreement with summer trends in the HadCM3 climate-model simulation that is driven with twentieth-century forcing and extended with anthropogenic forcing from 2000 on (Supplementary Fig. S2), the recent acceleration of summer trends is probably caused by anthropogenic influences (see ref. 10).

To interpret which individual forcings contribute to the detected fingerprints we applied a multifingerprint analysis[15] (see Methods). We used fingerprints for the response to individual forcings based on simple energy balance models (EBMs), as individual-forcing AOGCM runs were not consistently available. EBMs seem to show reasonable annual response to forcing on hemispheric scales[15], but miss dynamical responses[13], which would particularly affect the response in the cold season[21]. Results of the multifingerprint analysis show that a significant ($p < 5\%$) part of the increase in average European winter temperatures can be attributed to anthropogenic forcing (Fig. 2; best guess 90%, with large uncertainty ranges), although the response to volcanic and solar forcing is not distinguishable from European random climate variability on the basis of this analysis. The multifingerprint analysis for summer suggests a detectable solar signal (Fig. 2c), which is, however, not robust with respect to changes in the period analysed (see Supplementary Information). We analysed the role of solar forcing in summer further by applying a stepwise regression of the reconstruction and model data onto the time series of response to solar forcing. This method first removes the better-constrained greenhouse-gas response (see Methods), and then determines the spatial pattern in response to solar forcing[22]. The resulting spatial pattern in both models and reconstruction shows

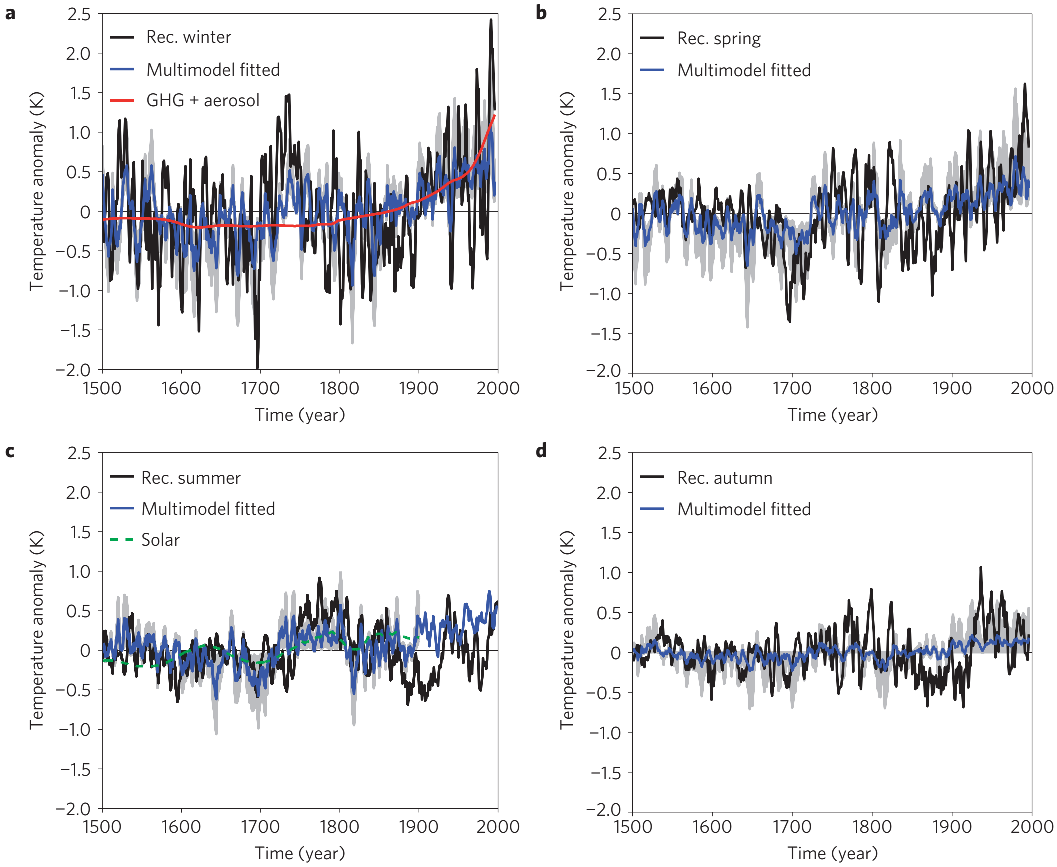

Figure 2 | Results from detection and attribution analysis of European mean temperatures. a–d, The multimodel mean fingerprint, scaled to the observations, is shown in blue. It is surrounded by an uncertainty range based on the fingerprint scaled over its 5–95% uncertainty range (grey). Winter (**a**), spring (**b**) and autumn (**d**) show a (5%) significant response to the fingerprint for external forcing. The fingerprint is detectable (<5% significant) in summer only for the pre-1900 period (**c**, scaling based on that period). All data are smoothed with a running 5 yr window. Detectable fingerprints in response to individual forcings, based on EBM simulations, are shown as thin lines in **a** and **c** (not robust).

continental-scale warming (see Supplementary Fig. S7; fingerprint 90% significant). However, this detection of the solar response is not robust to removing both volcanic and anthropogenic influence before the analysis, both of which are less uncertain than solar forcing[3]. Thus, solar influence on European summer temperatures remains speculative.

To identify to what extent European temperatures respond to volcanic eruptions, we carried out a superposed epoch analysis[11,19,21] (see Methods). We used several datasets to identify strong volcanic eruptions: a collection of large tropical volcanic eruptions (15 eruptions since 1500, and 10 since 1675) as used in ref. 21; a collection of six tropical volcanic eruptions, whose seasonal timing was likely to cause strong tropical stratospheric warming affecting the Northern Hemisphere in the following winter, and a larger number of years preceding sudden increases of aerosol optical depth (33 events since 1500, and 17 since 1675; ref. 23). Irrespective of which dataset of past volcanism was used, we find fairly good agreement between the reconstruction and the multimodel response following volcanic events (Fig. 3, which is based on 17 events post 1675; for figures for other cases and significance tables see Supplementary Information). The one or two winters following the eruptions show, on average, significant warming, similar to reported findings[11,21]. Winter warming is simulated by each model, and the agreement with the models is somewhat surprising given concern about the lack of dynamic response to volcanism in the winter season in climate models[8] and the underestimated response of the Northern Annular mode to forcing in the late twentieth century[3]. However, the signal-to-noise ratio of this winter warming is rather low. The spatial pattern of the multimodel volcanic fingerprint can only be detected at the 5% significance level in the first winter following a strong tropical eruption, and most robustly for the fingerprint of the first two winters combined in the case of the larger number of events (Fig. 3, bottom). This demonstrates that volcanic winter warming is a subtle change in the probability of a Northern European warming pattern, rather than a deterministic feature. Analyses focusing on the evolution of annual Northern Hemispheric, rather than European, temperatures have shown that volcanic forcing has contributed to cold conditions during the late sixteenth to early nineteenth century[15,19,24]. This is consistent with overall cold conditions in European winters during times of strong cumulative volcanic forcing (see Supplementary Information).

Summers immediately following volcanic eruptions are on average significantly colder than the preceding summers[21], and their fingerprint is detectable, irrespective of details of the analysis (Fig. 3). This indicates that volcanic eruptions with stratospheric aerosol forcing lead to highly significant and predictable cooling in European summer temperatures. Volcanic signals are not detectable in spring and autumn temperatures.

In conclusion, we find that European temperatures have been significantly influenced by external forcing in the past. Over the full 500 year period, a substantial fraction (25% for winter and spring, and 35% for annual temperatures, Table 1) of the interdecadal variance (that is, the variance in 11 yr smoothed data) was externally driven. Thus, the role of external forcing is weaker for Europe compared with hemispheric means (where a best estimate is that

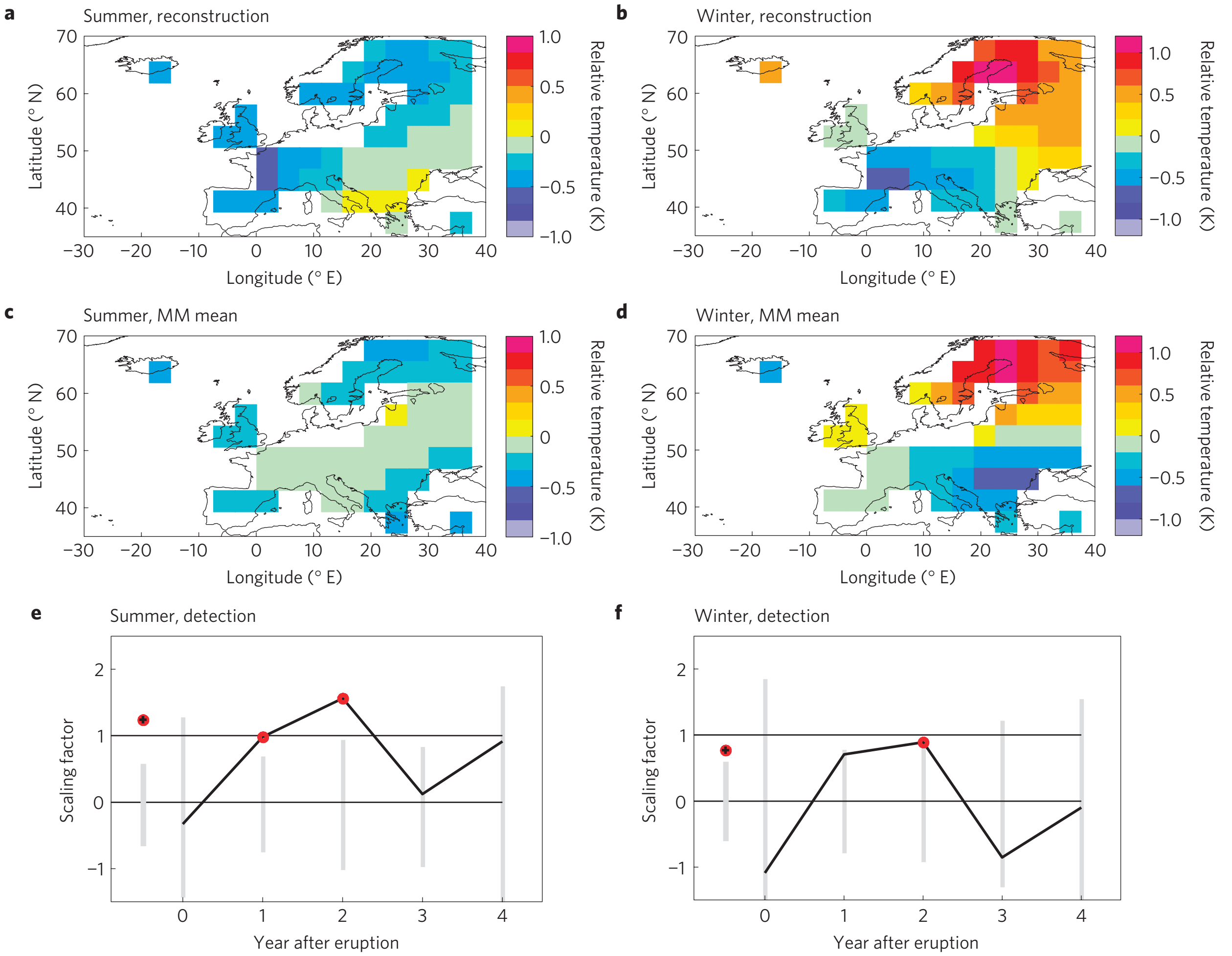

Figure 3 | Detection of fingerprints for volcanic forcing. a–f, Response to volcanic eruptions in summer (left) and winter (right). **a–d**, Average seasonal temperature pattern (K) in the year following a volcanic eruption relative to the preceding 5 years for the reconstruction (**a**,**b**) and the multimodel mean (**c**,**d**), using 17 eruptions since 1675. **e**,**f**, Scaling factors based on a regression of the response from the reconstruction on that from the multimodel mean for the year of the eruption (labelled zero), for the four following years and for years one and two combined (plotted at −0.5). A 5–95% significance range for scaling factors due to noise for each year, and years 1–2 combined (plotted at −0.5), is given by vertical grey bars; cases where the response is significant are marked by a red dot.

52–70% of variance over the past seven centuries is forced[15]). Nevertheless, much of the long-term variability in European mean winter and spring temperatures even before 1900 is reproduced by simulations driven with all forcings (Fig. 2), although it can only be detected if at least part of the twentieth-century warming is included in the analysis. In summer, external influence is detectable in the period 1500–1900. In addition, both winter and summer show a significant, but short-term, warming and cooling respectively following volcanic eruptions. Nevertheless, European winters are cold during times of strong cumulative volcanic forcing. Our results highlight the important role of radiative forcing even on regional scales, and indicate that present large radiative forcings will cause highly significant changes in European temperatures in the future. They also emphasize substantial differences in the response to forcing between seasons, which are important when predicting impacts.

Methods

Fingerprints for the effect of external forcings on European average temperature have been derived from three climate-model simulations of the last millennium. All model data were transformed to the ~3.75° × 3.75° grid of the coarser-resolution models (ECHO-G and NCAR-CSM1.4), using the land–sea mask of ECHO-G. We used fingerprints for total forcing $f_{\mathrm{tot}}(t)$ in time, averaging the land data of model and reconstruction, and applied a 5 yr running mean to reduce short-term variability in the resulting time series (results are robust to changes, for example using an 11 yr running mean instead). We use a total least square approach[25] to estimate the contribution of external forcing to European mean temperature $T_{\mathrm{Europe}}(t)$

$$T_{\mathrm{Europe}}(t) = \beta_{\mathrm{tot}}(f_{\mathrm{tot}}(t) + \varepsilon_{\mathrm{finger}}(t)) + \varepsilon_{\mathrm{noise}}(t) \quad (1)$$

where $\varepsilon_{\mathrm{noise}}$ is a residual associated with internal climate variability and $\varepsilon_{\mathrm{finger}}$ is variability superimposed on the fingerprint (note that an average of three AOGCM simulations will still be affected by climate variability). The uncertainty in scaling factors β_{tot} is assessed by using samples of random climate variability superimposed on the observations and then determining the 5–95% uncertainty range from scaling factors obtained for these samples. We use both the residual variability of the reconstruction and the variability of climate model simulations, after subtracting the response to all forcings combined, as samples of internal climate variability (see Supplementary Information).

Where the 5–95% range of scaling factors is above zero, we conclude that the fingerprint for external forcing is detected ($p < 5\%$) because its amplitude is unlikely to have been caused by internal climate variability alone (note that we use a one-sided test, because only positive scaling factors are consistent with the expected response). The total least square approach requires setting the ratio of noise variance between fingerprint and reconstruction. We chose a value of 1:3 to account for the reduction of noise variance from averaging the three model simulations by a factor of three. To determine uncertainty in β_{tot} we chose a ratio of 1:6, because the addition of random noise realizations to the observation doubles the variance of the noise in the reconstruction relative to the fingerprint. Results of all seasons but autumn were robust to using a simpler ordinary least square approach (see Supplementary Information). Note that error in reconstructions will generally make detection of a forced change more difficult and lead to conservative results, and that errors in the magnitudes of individual eruptions have little effect on the estimated response to volcanic eruptions[26].

Fingerprints for the role of individual forcings were not consistently available from the models. To clarify the relative role of individual forcings, we have attempted to separate them using time series of hemispheric mean temperature from EBM simulations[13]. The reconstruction was simultaneously regressed on the EBM simulation for the anthropogenic f_{anthro}, volcanic f_{vol} and solar f_{sol} fingerprints (equation (2)); note that the scaling factors $\beta_{\mathrm{sol}}, \beta_{\mathrm{vol}}, \beta_{\mathrm{anthro}}$ are now determined by an ordinary least square approach. This is appropriate because the EBM provides noise-free fingerprints:

$$T_{\mathrm{Europe}}(t) = \beta_{\mathrm{sol}} f_{\mathrm{sol}}(t) + \beta_{\mathrm{vol}} f_{\mathrm{vol}}(t) + \beta_{\mathrm{anthro}} f_{\mathrm{anthro}}(t) + \varepsilon_{\mathrm{noise}}(t) \quad (2)$$

We estimate the amplitudes of the fingerprints and the residual climate variability $\varepsilon_{\mathrm{noise}}$ simultaneously from the proxy reconstruction from 1500, and the 5–95% uncertainty in scaling factors is determined by applying the methods to time series from noise only and superimposing the resulting uncertainty range on the best-guess scaling factor[15].

We also use a superposed epoch analysis to determine the average short-term response to volcanic eruptions[19,21]. The response from multiple volcanic eruptions relative to the average of the preceding five non-volcanic years is averaged, and the significance is determined by repeating the analysis, using the same number of years chosen randomly from the whole record of the analysis. In both cases, the data are only analysed up to the next eruption. To determine if the model-simulated fingerprint of volcanic eruptions is significantly detectable, the spatial pattern resulting from the epoch analysis for the reconstructions has been regressed onto the epoch fingerprint pattern from the multimodel mean, both for individual years and for the two years immediately following an eruption combined to a time-space fingerprint. Significance is again determined by regressing results from an epoch analysis, where years from the reconstruction were chosen randomly rather than following known volcanic events, onto the model fingerprint pattern.

To determine the temperature pattern in response to solar forcing, European temperature patterns from models and reconstruction have been regressed on a temporal fingerprint for solar forcing. This fingerprint for solar forcing is based on an EBM run forced with the solar time series of Lean *et al.*[27], which was spliced with solar-forcing estimates for earlier times based on cosmogenic isotopes[28]. To avoid cross-contamination by the anthropogenic increase in CO_2, we used a solar-forcing fingerprint in time that is orthogonalized to that of anthropogenic forcing (see Supplementary Fig. S6). This is consistent with stepwise regression of the reconstruction onto first an anthropogenic, then a solar signal, consistent with the greater confidence in the shape and size of the greenhouse-gas and aerosol forcing[29]. In a final step, the solar fingerprint has been orthogonalized to both anthropogenic and volcanic forcing.

Received 29 June 2010; accepted 1 December 2010; published online 16 January 2011

References

1. Parry, M. L., Canziani, O. F., Palutikof, J. P., van der Linden, P. J. & Hanson, C. E. (eds) *IPCC Climate Change 2007: Impacts, Adaptation and Vulnerability* 976 (Cambridge Univ. Press, 2007) (http://www.cambridge.org/features/earth_environmental/climatechange/wg2.htm).
2. Stott, P. Attribution of regional-scale temperature changes to anthropogenic and natural causes. *Geophys. Res. Lett.* **30,** 1728–1731 (2003).
3. Hegerl, G. C. *et al.* in *IPCC Climate Change 2007: The Physical Science Basis* (ed. Solomon, S.) 663–745 (Cambridge Univ. Press, 2007).
4. Bengtsson, L., Hodges, K. I., Roeckner, E. & Brokopf, R. On the natural variability of the pre-industrial European climate. *Clim. Dyn.* **27,** 734–760 (2006).
5. Luterbacher, J., Dietrich, D., Xoplaki, E., Grosjean, M. & Wanner, H. European seasonal and annual temperature variability, trends and extremes since 1500. *Science* **303,** 1499–1503 (2004).
6. Xoplaki, E. *et al.* European spring and autumn temperature variability and change of extremes over the last half millennium. *Geophys. Res. Lett.* **32,** L15713 (2005).
7. Zorita, E. *et al.* Climate evolution in the last five centuries simulated by an atmosphere–ocean model: Global temperatures, the North Atlantic oscillation and the Late Maunder minimum. *Meteorol. Z.* **13,** 271–289 (2004).
8. Tett, S. F. B. *et al.* The impact of natural and anthropogenic forcings on climate and hydrology since 1550. *Clim. Dyn.* **28,** 3–34 (2007).
9. Ammann, C. *et al.* Solar influence on climate during the past millennium: Results from transient simulations with the NCAR Climate System Model. *Proc. Natl Acad. Sci. USA* **104,** 3713–3718 (2007).
10. Christidis, N., Stott, P. A., Jones, G. S., Shiogama, H., Nozawa, T. & Luterbacher, J. 2010: Human activity and warm seasons in Europe. *Int. J. Climatol.* doi:10.1002/joc.2262 (in the press).
11. Jones, P. *et al.* High-resolution palaeoclimatology of the last millennium: A review of current status and future prospects. *Holocene* **19,** 3–49 (2009).
12. Mann, M. *et al.* Global signatures and dynamical origins of the Little Ice Age and Medieval Climate Anomaly. *Science* **326,** 1256–1260 (2009).
13. Shindell, D., Schmidt, G., Miller, R. & Mann, M. Volcanic and solar forcing of climate change during the preindustrial era. *J. Clim.* **16,** 4094–4107 (2003).
14. Zorita, E., González-Rouco, J. F., von Storch, H., Montávez, J. P. & Valero, F. Natural and anthropogenic modes of surface temperature variations in the last thousand years. *Geophys. Res. Lett.* **32,** L08707 (2005).
15. Hegerl, G. C. *et al.* Detection of human influence on a new 1500 yr climate reconstruction. *J. Clim.* **20,** 650–666 (2007).
16. Küttel, M. *et al.* Testing a European winter surface temperature reconstruction in a surrogate climate. *Geophys. Res. Lett.* **34,** L07710 (2007).
17. Lee, T. C. K., Zwiers, F. W. & Tsao, M. Evaluation of millennial proxy reconstruction methods. *Clim. Dyn.* **31,** 263–281 (2008).
18. González-Rouco, J. F., von Storch, H. & Zorita, E. Deep soil temperature as a proxy for surface air-temperature in a coupled model simulation of the last thousand years. *Geophys. Res. Lett.* **30,** 2116–2119 (2003).
19. Hegerl, G. C., Crowley, T. J., Baum, S. K., Kim, K. Y. & Hyde, W. T. Detection of volcanic, solar and greenhouse gas signals in paleo-reconstructions of Northern Hemispheric temperature. *Geophys. Res. Lett.* **30,** 1242–1245 (2003).
20. Goosse, H. *et al.* The origin of the medieval warm period. *Clim. Past* **2,** 99–113 (2006).
21. Fischer, E. M. *et al.* European climate response to tropical volcanic eruptions over the last half millennium. *Geophys. Res. Lett.* **34,** L05707 (2007).
22. Weber, S. L., Crowley, T. J. & van der Schrier, G. Solar irradiance forcing of centennial climate variability during the Holocene. *Clim. Dyn.* **22,** 539–553 (2004).
23. Crowley, T. J. *et al.* Volcanism and the little ice age. *PAGES News* **16,** 22–23 (2008).
24. Yoshimori, M., Stocker, T. F., Raible, C. C. & Renold, M. Externally forced and internal variability in ensemble climate simulations of the Maunder minimum. *J. Clim.* **18,** 4253–4270 (2005).
25. Allen, M. R. & Stott, P. A. Estimating signal amplitudes in optimal fingerprinting, Part I: Theory. *Clim. Dyn.* **21,** 477–491 (2003).
26. Hegerl, G. C., Crowley, T. J., Hyde, W. T. & Frame, D. Climate sensitivity constrained by temperature reconstructions of the last seven centuries. *Nature* **440,** 1029–1032 (2006).
27. Lean, J. L., Wang, Y. M. & Sheeley, N. R. The effect of increasing solar activity on the Sun's total and open magnetic flux during multiple cycles: Implications for solar forcing of climate. *Geophys. Res. Lett.* **29,** 2224–2227 (2002).
28. Crowley, T. J. Causes of climate change over the past 1000 years. *Science* **289,** 270–277 (2000).
29. Hegerl, G. C. & Allen, M. R. Origins of model-data discrepancies in optimal fingerprinting. *J. Clim.* **15,** 1348–1356 (2002).
30. Brohan, P., Kennedy, J. J., Harris, I, Tett, S. F. B. & Jones, P. D. Uncertainty estimates in regional and global observed temperature changes: A new dataset from 1850. *J. Geophys. Res.* **111,** D12106 (2006).

Acknowledgements

We thank E. Zorita and C. Ammann for help with data from the ECHO-G and CCSM models. We thank A. Schurer, A. Bozzo and M. Küttel for comments and discussion and three anonymous reviewers for their constructive comments. The publication was supported by NSF grant ATM-0296007, NERC grant NE/G019819/1 and NCAS. E.X. and J.L. acknowledge support by the EU/FP6 integrated project CIRCE (NO036961) and from the EU/FP7 project ACQWA (NO212250). J.L. also acknowledges support from the DFG Projects PRIME ('Precipitation in the past millennium in Europe') within the Priority Programme 'INTERDYNAMIK' and 'Historical climatology of the Middle East based on Arabic sources back to AD 800'.

Author contributions

G.H. and J.L. discussed and planned the work; G.H. carried out the analysis; J.L. and E.X. provided the reconstruction; F.G-R., E.X. and S.F.B.T. provided model data and comments/text, and T.C. provided his volcanic reconstructions and its interpretation as well as overall comments. All authors contributed to discussion, interpretation and writing of the paper.

Additional information

The authors declare no competing financial interests. Supplementary information accompanies this paper on www.nature.com/naturegeoscience. Reprints and permissions information is available online at http://npg.nature.com/reprintsandpermissions. Correspondence and requests for materials should be addressed to G.H.